Development 137, 1339-1349 (2010) doi:10.1242/dev.044610

Direct activation of *Shroom3* transcription by Pitx proteins drives epithelial morphogenesis in the developing gut

Mei-I Chung[1], Nanette M. Nascone-Yoder[2], Stephanie A. Grover[3], Thomas A. Drysdale[3,4,5] and John B. Wallingford[1,6,*]

SUMMARY

Individual cell shape changes are essential for epithelial morphogenesis. A transcriptional network for epithelial cell shape change is emerging in *Drosophila*, but this area remains largely unexplored in vertebrates. The distinction is important as so far, key downstream effectors of cell shape change in *Drosophila* appear not to be conserved. Rather, Shroom3 has emerged as a central effector of epithelial morphogenesis in vertebrates, driving both actin- and microtubule-based cell shape changes. To date, the morphogenetic role of Shroom3 has been explored only in the neural epithelium, so the broad expression of this gene raises two important questions: what are the requirements for Shroom3 in non-neural tissues and what factors control *Shroom3* transcription? Here, we show in *Xenopus* that Shroom3 is essential for cell shape changes and morphogenesis in the developing vertebrate gut and that *Shroom3* transcription in the gut requires the Pitx1 transcription factor. Moreover, we show that Pitx proteins directly activate *Shroom3* transcription, and we identify Pitx-responsive regulatory elements in the genomic DNA upstream of *Shroom3*. Finally, we show that ectopic expression of Pitx proteins is sufficient to induce Shroom3-dependent cytoskeletal reorganization and epithelial cell shape change. These data demonstrate new breadth to the requirements for Shroom3 in morphogenesis, and they also provide a cell-biological basis for the role of Pitx transcription factors in morphogenesis. More generally, these results provide a foundation for deciphering the transcriptional network that underlies epithelial cell shape change in developing vertebrates.

KEY WORDS: Pitx1, Pitx2, Shroom, Apical constriction, Epithelium, Gut, *Xenopus*

INTRODUCTION

As embryos develop, they undergo a successive series of dynamic morphological changes that generate their final shape. Such tissue movements are driven by a variety of morphogenetic engines, including cell rearrangements, oriented cell divisions and changes in cell shape. Cell shape changes are of particular importance during the morphogenesis of epithelial sheets, in which bending is facilitated by the specific constriction of the apical surfaces of cells (Burnside and Jacobson, 1968; Jacobson and Gordon, 1976; Leptin and Grunewald, 1990; Schoenwolf, 1988). Interestingly, cells undergoing such apical constriction are almost universally characterized by elongation along their apicobasal axis (Burnside, 1973; Sweeton et al., 1991; Viamontes and Kirk, 1977). Moreover, such apicobasal cell elongation may play a crucial morphogenetic role even in the absence of apical constriction, as many epithelial sheets thicken without bending (Burnside, 1973; Schoenwolf, 1991). Recent studies have begun to identify the cytoskeletal regulators of such cell shape changes.

[1]Section of Molecular Cell and Developmental Biology, University of Texas at Austin, Austin, TX 78712, USA. [2]Department of Molecular Biomedical Sciences, Center for Comparative Medicine and Translational Research, College of Veterinary Medicine, North Carolina State University, Raleigh, NC 27606, USA. [3]Children's Health Research Institute, 800 Commissioners Rd. E. London, Department of Biology, University of Western Ontario, Ontario, N6C 2V5, Canada. [4]Department of Pediatrics, University of Western Ontario, Ontario, N6C 2V5, Canada. [5]Department of Physiology and Pharmacology, University of Western Ontario, Ontario, N6C 2V5, Canada.[6]Howard Hughes Medical Institute, University of Texas at Austin, Austin, TX 78712, USA.

*Author for correspondence (wallingford@mail.utexas.edu)

Accepted 1 February 2010

In vertebrates, a central regulator of morphogenetic cell shape changes is Shroom3, a protein that is essential for neural tube closure in mouse, *Xenopus* and chick (Haigo et al., 2003; Hildebrand and Soriano, 1999; Nishimura and Takeichi, 2008). Shroom3 is necessary for both apicobasal cell elongation and apical constriction in the neural epithelium (Haigo et al., 2003; Lee et al., 2007). Curiously, although Shroom3 acts via the actin cytoskeleton to drive apical constriction, it appears that Shroom family proteins control apicobasal cell elongation by repositioning the microtubule nucleator γ-tubulin (Fairbank et al., 2006; Haigo et al., 2003; Hildebrand, 2005; Lee et al., 2007; Nishimura and Takeichi, 2008). How a single protein acts to govern multiple cytoskeletal rearrangements remains unclear, but Shroom3 function has been shown to involve several effector proteins, including Mena (also known as Enah), myosin II, the Rap1 GTPase and Rho kinase (Haigo et al., 2003; Hildebrand, 2005; Hildebrand and Soriano, 1999; Lee et al., 2007; Nishimura and Takeichi, 2008; Plageman et al., 2010). Although it is clear that Shroom3 is central to epithelial cell shape change in vertebrates, several important issues remain unresolved.

First, epithelial cell shape changes in vertebrates have only been studied in any detail in the folding epithelium of the neural plate, where Shroom3 is essential. However, apical constriction and cell elongation are observed in several morphogenetically active epithelial tissues. Indeed, Shroom3 is expressed in several thickened epithelial sheets (Lee et al., 2009), but its function in these tissues has not been tested experimentally. Of particular interest is the gut, where complex changes in the thickness of cell sheets are important for morphogenesis (Chalmers and Slack, 1998; Davis et al., 2008; Muller et al., 2003; Reed et al., 2009). Interestingly, the cell rearrangements that shape the posterior gut appear not to act anteriorly (Larkin and Danilchik, 1999; Li et al., 2008). Thus, cell

shape changes might be of particular importance in the anterior gut. *Shroom3* mutant mice display gross gastroschisis (Hildebrand and Soriano, 1999), but whether or not Shroom3 controls cell shape changes during gut morphogenesis remains an important and unanswered question.

A second crucial question concerns transcriptional regulation of cell shape change in vertebrates. Indeed, although transcriptional control of epithelial cell shape change has been studied in *Drosophila* (e.g. Kolsch et al., 2007; Morize et al., 1998), it remains largely unstudied in vertebrates. Understanding the links between transcriptional regulation and cytoskeletal activity will be central to understanding developmental tissue morphogenesis. Tantalizing candidates for transcriptional control of *Shroom3* are the Pitx family of transcription factors (Gage et al., 1999b), as Pitx2 is required for left-right asymmetric morphogenesis, and its expression has been correlated with changes in cell shape (Davis et al., 2008; Rodriguez-Leon et al., 2008). However, nothing is yet known about the transcriptional targets of Pitx proteins that might mediate epithelial morphogenesis.

Here, we address these two open questions regarding vertebrate epithelial cell shape change. First, we report that Shroom3 is expressed in the epithelium of the developing gut in *Xenopus* and that it is required for cell shape changes and morphogenesis in this tissue. We then show that *Shroom3* expression in the gut is under the control of Pitx1 and, moreover, that Pitx1 is required for gut morphogenesis. To link these two findings, we show that Pitx transcription factors can directly activate *Shroom3* transcription via Pitx-responsive regulatory elements in the genomic DNA upstream of *Shroom3*. Finally, we show that ectopic expression of Pitx transcription factors in epithelial cells is sufficient to induce Shroom3-dependent apical constriction, apicobasal cell elongation and microtubule assembly. Pitx transcription factors can drive these cell shape changes without activating transcription of the known Shroom3 effectors. These data therefore define a surprisingly direct genetic system that is necessary and sufficient to initiate epithelial cell shape changes that drive gut morphogenesis in a vertebrate.

MATERIALS AND METHODS

Collection and manipulation of embryos

Manipulations of *Xenopus* embryos were performed as described (Sive et al., 2000). Female *Xenopus laevis* were injected with 700 μl of human chorionic gonadotropin hormone (HCG) and kept at 18°C overnight. The next day, eggs were isolated and fertilized. Embryos were de-jellied using a 3% cysteine solution in 1/3× MMR.

Morpholino and mRNA injection

Capped mRNA was synthesized using mMESSAGE mMACHINE (Ambion). mRNA was injected into one ventral blastomere at the 4-cell stage. Antisense morpholino oligonucleotide (MO) was injected into the D2.1 blastomere at the 16-cell stage (Moody and Kline, 1990). Embryos were incubated until appropriate stages (Nieuwkoop and Faber, 1967) and were fixed in MEMFA (Davidson and Wallingford, 2005; Sive et al., 2000). Embryos were embedded in 2% agarose and thick (250-300 μm) sections were cut with a Vibratome series 1000 (Davidson and Wallingford, 2005).

The Shroom3 MO was used as previously described (Haigo et al., 2003; Lee et al., 2007). This MO effectively blocks splicing of the *Shroom3* transcript and is phenocopied in all tested assays by expression of a dominant-negative Shroom3 construct (Haigo et al., 2003; Lee et al., 2007).

Two Pitx1 MOs were used, one blocking translation (5′-CATGGTCAATCACTTCTGCTCATGA-3′, 50 ng), the other splicing (5′-CTTTCTCTGTCAAACATATCAAGAT-3′, 60 ng).

Immunohistochemistry

Immunostaining was performed as described (Lee et al., 2008). Briefly, fixed embryos were dehydrated completely in methanol and were bleached in 10% hydrogen peroxide/67% methanol for 3 hours and rehydrated consecutively with TBS (155 mM NaCl, 10 mM Tris-Cl, pH 7.4). To reduce autofluorescence of yolk platelets, the embryos were incubated with 100 mM $NaBH_4$ in TBS for 4 hours at room temperature or overnight at 4°C and rinsed in TBST (0.1% Triton X-100 in TBS). In some cases, Eriochrome or Sudan Black was used to reduce autofluorescence as described (Reed et al., 2009).

Primary antibodies used were monoclonal anti-α-tubulin (1:300 dilution, clone DM1A, Sigma), rabbit polyclonal anti-γ-tubulin (1:200, Abcam), rabbit anti-GFP (1:500, Invitrogen) and polyclonal rabbit anti-ZO-1 (1:200, Zymed Laboratories).

Antibodies were diluted in fetal bovine serum (FBS) solution (TBS containing 10% FBS and 5% DMSO). Primary antibodies were detected with Alexa Fluor 488 goat anti-mouse IgG or Alexa Fluor 555 goat anti-rabbit IgG (both Molecular Probes) diluted 1:300 in FBS solution. Embryos were cleared in Murray's Clear solution (2:1 benzyl benzoate:benzyl alcohol). Images were obtained using a Zeiss LSM5 Pascal confocal microscope. Cell heights were measured using LSM5 Pascal software. Archenteron floor angle and thickness were measured with Image-Pro Plus software (Media Cybernetics). Some of the images shown have been processed using the Unsharp Mask filter in Adobe Photoshop.

In situ hybridization

In situ hybridization was performed as described previously (Sive et al., 2000). The images and fluorescence view were captured on a Leica MZ16FA fluorescence stereomicroscope. To observe cell morphology, embryos were then immunostained for α-tubulin and imaged as described above.

Animal cap explants and reverse transcription PCR

Pitx1 mRNA or *Pitx1-GR* mRNA (100 pg) was injected into the animal pole at the 4-cell stage. Animal cap explants were dissected at stage 8 and cultured as described previously (Sive et al., 2000). *Pitx1-GR*-injected explants were treated with 10 μM dexamethasone (Sigma) after a 10-minute pretreatment with 10 μg/ml cycloheximide (Sigma) and cultured to the appropriate stage. Twenty explants of each sample were collected for the preparation of cDNA. PCR was performed and relative expression intensities determined by analyzing band intensities with ImageJ software (NIH).

PCR was performed with the following primers (5′ to 3′, forward and reverse):
Shroom3, AGGATGAGGGTGACGATGAG and CAAGCCCTCCATTAAGTCCA;
Shroom1, TCTGGAGAAAGTGGTGAGCCTG and TCATTTGTAGCGGGTGGACG;
Xag1, CTGACTGTCCGATCAG and CTTAGAGATGGAGAAGTGTGC;
MyoIIb, TGCTGCACAATCTGAAGGAC and TCGGATAAATTTGCCAAAGC;
Mena, AGCGACAGAAGGAGTTGGAAC and GAATCTTCATTCCGGGACACTT;
Rap1a, GCTCAGGAGGTGTTGGAAAG and AGCAGCAGACATTTTGGTTTC;
Rap1b, GGAACGGAACAATTCACAGC and CACCACAGGAAAGTCCATTG;
Rock1, AAACGAGCTCCAGATGCAGT and TGACATGGCATTTTCGACATTC;
Rock2, GCCAAAAAGTTTGGTTGGAA and TTGGGGATCTTTTTCACCAG; and
Efl1α, CAGATTGGTGCTGGATATGC and ACTGCCTTGATGACTCCTAG.

Luciferase reporter assay

Embryos were injected at the 4-cell stage in each blastomere with 100 pg luciferase reporter constructs and pRL-TK vector, with or without 100 pg *Pitx1* mRNA. For each sample, three pools of five embryos were collected at stage 12 and dual-luciferase assays were performed as described (Promega). Firefly luciferase activity was normalized to *Renilla* luciferase activity in each sample.

RESULTS

Shroom3 is essential for morphogenesis in the developing vertebrate gut

Given the ability of Shroom3 to direct epithelial cell shape change, we first asked whether Shroom3 was expressed in the developing gut, where changes in cell shape are correlated with morphogenesis. To explore this issue, we exploited embryos of *Xenopus laevis*; the large size of *Xenopus* embryos and cells makes this animal an outstanding tetrapod model with which to examine the cell-biological basis of tissue morphogenesis. Indeed, we found that *Shroom3* was expressed strongly and widely throughout the developing gut, with particularly intense expression in the foregut and the caudal hindgut at later stages (Fig. 1A; see Fig. S1 in the supplementary material).

To examine whether Shroom3 plays a general role in gut morphogenesis, we disrupted its function using a well-characterized dominant-negative construct, Shroom3$^{745\text{-}1108}$ (DN-Shrm3) (Haigo et al., 2003; Lee et al., 2007). Using targeted microinjection (Muller et al., 2003), we delivered mRNAs encoding either GFP alone or GFP together with DN-Shrm3 specifically to the developing gut. The GFP-expressing guts elongated and coiled normally and GFP-positive cells within these control guts took on an apicobasally elongated, high-columnar morphology that was indistinguishable from neighboring, non-GFP-expressing cells in the gut epithelium (Fig. 1B,B′,D). By contrast, guts of embryos co-injected with DN-Shrm3 failed to properly elongate and coil (Fig. 1C,C′). Moreover, the GFP-positive cells in embryos co-expressing DN-Shrm3 were rounded in appearance and GFP-positive regions of the gut epithelium were noticeably disorganized (Fig. 1E). These defects were dose dependent (not shown). These data demonstrate a requirement for Shroom3 in gut morphogenesis in *Xenopus*. Shroom3 is similarly expressed in the fore- and hindgut of the mouse, and although *Shroom3* mutant mice display gross gastroschisis (Hildebrand and Soriano, 1999), that phenotype has not yet been examined in any detail. Our results thus suggest that Shroom3 might play a conserved role in vertebrate gut morphogenesis.

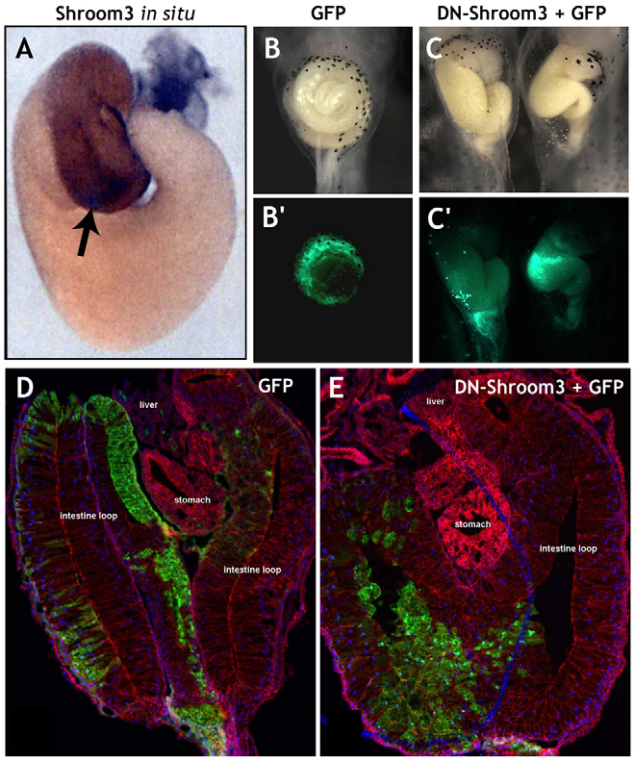

Fig. 1. Shroom3 is essential for morphogenesis of the developing *Xenopus* gut. (**A**) The expression pattern of *Shroom3* in a normal stage 43 dissected gut. *Shroom3* is robustly expressed in the foregut (arrow). (**B**,**B′**) Normal gut looping in a control stage 46 embryo injected with mRNA encoding GFP only (green in B′). (**C**,**C′**) Gut looping is disrupted following dominant-negative (DN)-Shroom3 expression (as marked by GFP, green in C′). (**D**,**E**) Control gut (D) and DN-Shroom3-injected (E) gut epithelium. GFP-positive gut epithelial cells display a high-columnar morphology in controls, whereas cells expressing GFP and DN-Shroom3 display more rounded shapes.

Shroom3 is essential for cell shape changes during gut morphogenesis

Shroom family proteins are known to be necessary and sufficient to drive cell shape changes in epithelial sheets, including apical constriction and apicobasal cell elongation (Haigo et al., 2003; Lee et al., 2009; Lee et al., 2007). However, the role of Shroom3 in controlling cell shape changes in non-neural tissues has not been explored in detail. Owing to the complex morphogenesis of the gut at later stages, we chose to examine the cell-biological role of Shroom3 in a less complex endodermal epithelium, the archenteron floor, where *Shroom3* is also strongly expressed (Fig. 2A,B).

The archenteron floor has a V-shaped morphology, and elongated, apically constricted cells are in evidence (Fig. 2C). To quantify the morphology of this tissue, we measured the angle at which the two sides of the epithelium intersect; in control embryos this angle was 81±5° (mean ± s.e.m.; n=10). We disrupted Shroom3 function by injection of an antisense morpholino oligonucleotide that effectively blocks splicing of the *Shroom3* mRNA (Shroom3 MO) (Haigo et al., 2003; Lee et al., 2007). Consistent with a role for Shroom3 in the apical constriction of these cells, injection of Shroom3 MO consistently resulted in loss of the V-shaped morphology of the archenteron floor (Fig. 2D); the average angle for morphants was significantly less acute, at 121±7° (P<0.001; n=20). Injection of control MO had no effect (not shown).

Shroom3 is essential for the assembly of apicobasally aligned microtubules (MTs) that contribute to cell shape changes in the neural epithelium (Lee et al., 2007). Accordingly, we observed that Shroom3 knockdown caused a marked reduction in MT assembly in epithelial cells of the archenteron floor in Shroom3 morphants (Fig. 2C,D). This reduction in MT assembly was accompanied by a 15% reduction in epithelial thickness, a difference that was highly significant (P=0.0003; n=13 controls, 21 morphants).

In neural tissues, Shroom3 knockdown results in a loss of γ-tubulin accumulation in cells that are actively changing shape, but does not affect the localization of the tight junction marker ZO-1 (also known as Tjp1) (Lee et al., 2007). We likewise observed that Shroom3 knockdown in the archenteron floor resulted in a loss of accumulated γ-tubulin, but localization of ZO-1 was not affected (Fig. 2E-H). It should be noted also, that the distance between ZO-1 signals revealed a failure of apical constriction in Shroom3 morphant epithelia (Fig. 2G,H). As in the neural tube, there was an apical accumulation of actin in the archenteron floor cells and this accumulation was dependent on Shroom3 activity (data not shown).

Together, these data thus reveal a role for Shroom3 in controlling cell shape change, cytoskeletal organization and tissue morphogenesis in the developing *Xenopus* endoderm. *Shroom3* mutant mice display a gross gut defect, but the cellular basis of that

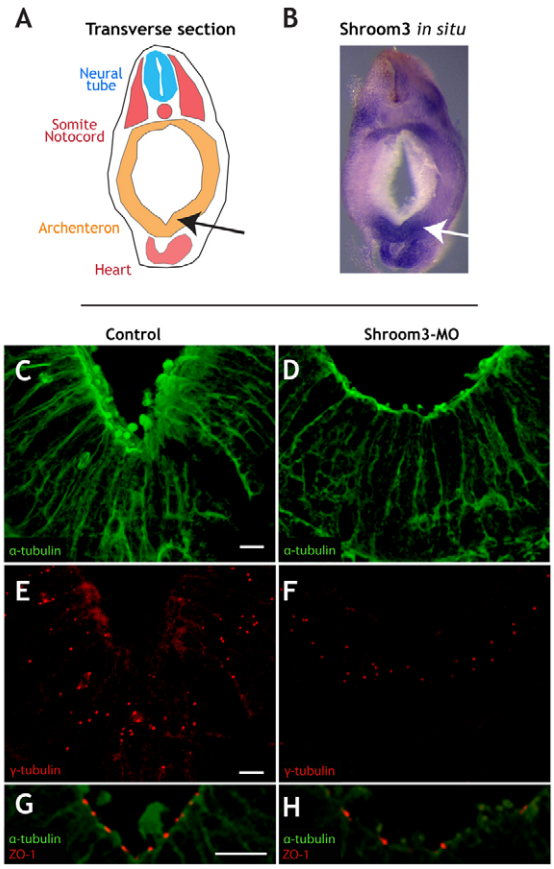

Fig. 2. Shroom3 is essential for cell shape change during gut morphogenesis. (**A**) Diagram of a transverse section of the stage 32 *Xenopus* embryo. (**B**) *Shroom3* expression in the endoderm at stage 32. Note the robust *Shroom3* expression (arrow) in the archenteron floor and roof. (**C**) α-tubulin staining of the archenteron floor in a control embryo. The archenteron floor displays a V-shaped morphology. (**D**) Archenteron floor morphology is disrupted and microtubule (MT) arrays are reduced in cells lacking Shroom3. We observed a less acute archenteron floor angle in Shroom3 MO-injected embryos (P=0.001, Mann-Whitney U-test). Moreover, archenteron floor thickness is reduced from 68±1 μm (mean ± s.e.m.; n=13) in control embryos to 59±1 μm (n=21) (P=0.0003) in Shroom3 MO-injected embryos. (**E**) γ-tubulin staining of the archenteron floor in a control embryo. (**F**) γ-tubulin accumulation is reduced in archenteron floor cells lacking Shroom3 function. (**G**) ZO-1 staining of tight junctions in archenteron floor cells. (**H**) The apical surface of archenteron floor cells is less constricted in the Shroom3 morphant embryo. ZO-1 localization is not affected. Scale bars: 10 μm.

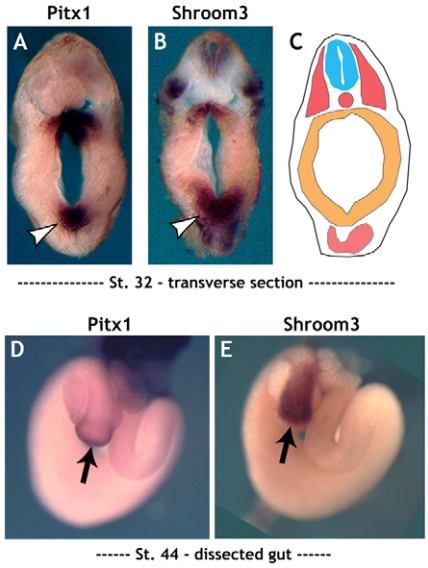

Fig. 3. Pitx1 and Shroom3 are co-expressed in the developing gut. (**A-C**) Expression patterns of (A) Pitx1 and (B) Shroom3 in a transverse section of the stage 32 *Xenopus* embryo, as schematized in C. Both Shroom3 and Pitx1 are expressed in the archenteron roof and floor (arrowheads). (**D**,**E**) At stage 44, a ventral view of dissected guts reveals that both (D) Pitx1 and (E) Shroom3 are expressed in the foregut (arrows).

defect has not been reported. Because the cell-biological basis of Shroom3 function in the neural plate is conserved between mice, frogs and chicken (Haigo et al., 2003; Hildebrand, 2005; Nishimura and Takeichi, 2008), our data argue that Shroom3 controls vertebrate gut morphogenesis by regulating epithelial cell shape changes.

Pitx1 controls Shroom3 expression in the developing gut

Shroom3 is sufficient to drive dramatic changes in cell shape even in the absence of nascent transcription (Haigo et al., 2003; Lee et al., 2007), so understanding the transcriptional regulation of *Shroom3* itself will be important. We noted that Shroom3 was co-expressed with Pitx1 in the developing endoderm. Both Shroom3 and Pitx1 were strongly expressed in the epithelium of the late archenteron, with intense expression in the archenteron roof and floor (Fig. 3A,B) (see Schweickert et al., 2001). At later stages, Pitx1 and Shroom3 were co-expressed, particularly in the foregut (Fig. 3D,E). This co-expression pattern was of interest to us because Shroom3 drives apicobasal cell elongation, and the apicobasal elongation of cells of the *Xenopus* gut varies along the anteroposterior axis (Chalmers and Slack, 1998). The co-expression data led us to ask whether Pitx1 governs *Shroom3* expression in the developing gut.

We inhibited Pitx1 function using MOs that disrupt translation of the mRNA. When assessed at early stages, targeted injection of the Pitx1 MO into the ventral endoderm resulted in a dramatic reduction of *Shroom3* expression in the archenteron floor (Fig. 4B, red arrow). The epithelium of the archenteron roof was not targeted by our injections, as monitored by co-injection of fluorescent dextran as a tracer (not shown), and *Shroom3* expression in such non-targeted regions was unaffected in experimental embryos (Fig. 4B). At later stages, when Shroom3 expression was evident in the foregut (Fig. 5A,C, black arrow), this expression was also clearly reduced following injection of the Pitx1 MO (Fig. 5B,D, red arrow). Finally, we performed RT-PCR on dissected guts, and observed a reduction in the level of *Shroom3* expression in morphant guts (data not shown). Injection of a 5-bp-mismatched Pitx1 MO had no effect on Shroom3 expression (not shown). These data suggest that Pitx1 is required for *Shroom3* transcription in the foregut.

Pitx1 is required for *Xenopus* gut morphogenesis

Since Pitx1 is required for *Shroom3* expression and Shroom3 is in turn required for gut morphogenesis, we predicted that Pitx1 knockdown should phenocopy the result of Shroom3 knockdown. Indeed, we observed that knockdown of Pitx1 with a translation-

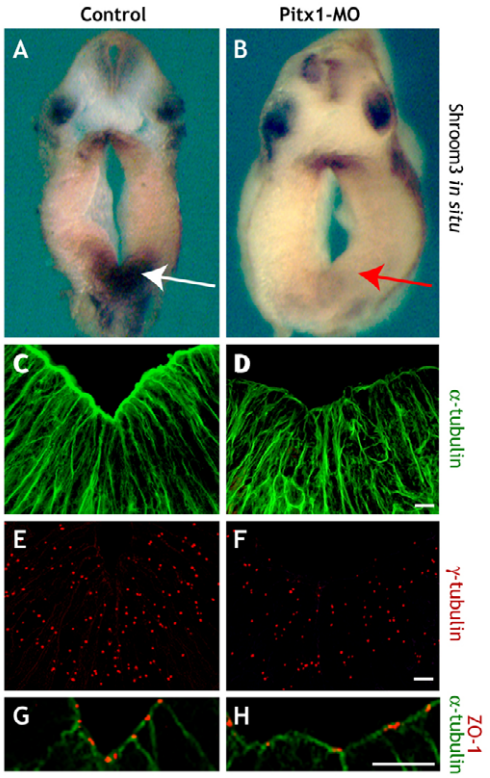

Fig. 4. Pitx1 controls Shroom3 expression in the developing gut. (**A**,**B**) Transverse sections showing *Shroom3* expression in (A) a control *Xenopus* embryo and (B) the Pitx1 MO-injected embryo, where *Shroom3* expression is reduced in the archenteron floor (arrows). The regions indicated by the arrows in A and B approximate to those shown at higher magnification in C,E and D,F, respectively. (**C**) α-tubulin staining of control archenteron floor cells. (**D**) α-tubulin staining of archenteron floor cells lacking Pitx1. The archenteron floor fails to take on its deep V-shaped morphology, showing an average archenteron floor angle 132±4° (mean ± s.e.m.; n=22), compared with 62±5° (n=16) (P<0.0001) in control embryos. Moreover, the archenteron thickness is reduced from 90±3 μm (mean ± s.e.m.; n=13) to 68±3 μm (n=17) (P<0.001). (**E**) γ-tubulin staining of the archenteron floor in the control embryo. (**F**) γ-tubulin accumulates less in archenteron floor cells lacking Pitx1. (**G**) ZO-1 staining of control archenteron floor cells. (**H**) The apical surface of archenteron floor cells is less constricted in the Pitx1 knockdown embryo, whereas ZO-1 localization is not affected. Scale bars: 10 μm.

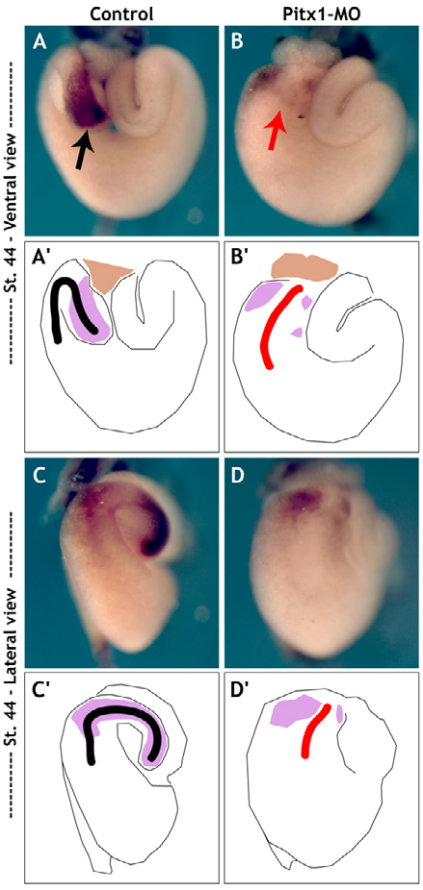

Fig. 5. Pitx1 is essential for *Xenopus* gut morphogenesis. (**A**,**A′**,**C**,**C′**) Ventral (A,A′) and lateral (C,C′) views of a stage 44 dissected control gut reveal Shroom3 expression in the foregut (arrow in A). In the diagrams, Shroom3 expression is represented in purple and normal gut looping by the black line. (**B**,**B′**,**D**,**D′**) Ventral (B,B′) and lateral (D,D′) views of dissected guts lacking Pitx1 reveal reduced Shroom3 expression in the foregut (arrow in B). The Pitx1 morphant displays a failure of looping (red line) in the foregut, corresponding to regions of disrupted Shroom3 expression.

blocking MO resulted in reduced apicobasal thickness and a failure of the archenteron floor to take on its normal, acutely bent morphology (Fig. 4C,D; control angle, 62±5°; morphant angle, 132±4°; P<0.001; n=16 controls, 22 morphants). Moreover, at later stages, Pitx1 morphants displayed a failure of elongation and looping in the foregut that corresponded to regions of reduced Shroom3 expression (Fig. 5B,B′,D,D′). Injection of the 5-bp-mismatched Pitx1 MO had no effect (not shown).

At the cellular level, we noted that cells of the archenteron floor in Pitx1 morphants, as compared with controls, failed to take on their narrow and apicobasally elongated morphology and failed to assemble robust apicobasally aligned MT bundles (Fig. 4D). In addition, Pitx1 morphants displayed a reduction in γ-tubulin accumulation, although ZO-1 localization was normal (Fig. 4E-H). As in Shroom3 morphants, the wide separation of ZO-1 signals revealed a defect in apical constriction in Pitx1 morphants (Fig. 4G,H).

Importantly, identical phenotypes were elicited by the translation-blocking MO and by a second MO designed to disrupt splicing of the *Pitx1* transcript (see Fig. S2 in the supplementary material). Thus, Pitx1 knockdown not only eliminates Shroom3 expression, but also recapitulates the phenotype of Shroom3 disruption in terms of tissue morphogenesis, cell shape and cytoskeletal organization.

Ectopic expression of Pitx1 activates Shroom3 expression

We noted that genes in the Pitx family were co-expressed with Shroom3 in tissues other than the gut, including the cement gland and the otic placodes (Lee et al., 2009; Lee et al., 2007; Pommereit et al., 2001; Schweickert et al., 2001). These findings led us to ask whether Shroom3 is a general target of the Pitx family of transcription factors. To this end, we generated mosaic embryos

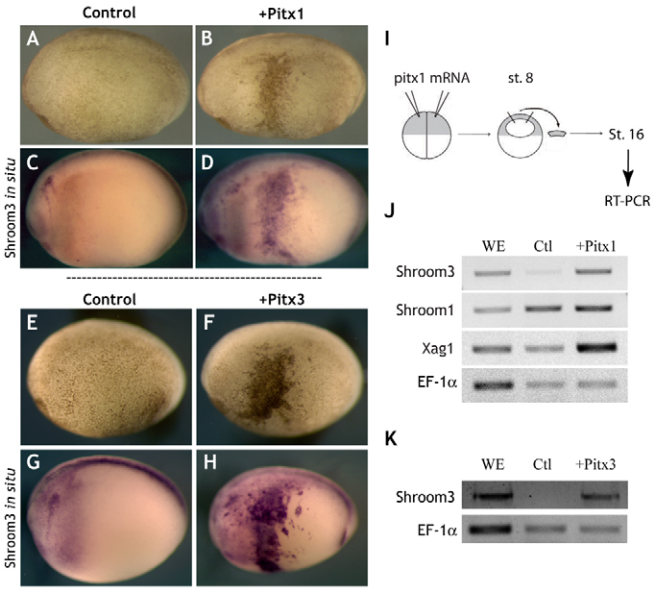

Fig. 6. Ectopic Pitx1 activates Shroom3 expression. (**A**) Stage 19 control *Xenopus* embryo. (**B**) Ectopic expression of Pitx1 in the epidermis induces ectopic pigment accumulation, similar to that induced by Shroom3 expression (Haigo et al., 2003; Lee et al., 2007). (**C**) *Shroom3* expression pattern in a control embryo. (**D**) Ectopic Pitx1 expression activates ectopic *Shroom3* expression in the epidermis. (**E**,**F**) Control (E) and *Pitx3*-injected (F) embryos. Ectopic Pitx3 also induces pigment accumulation. (**G**) Control *Shroom3* expression pattern. (**H**) Ectopic Pitx3 expression activates ectopic *Shroom3* expression in the epidermis. (**I**) Experimental scheme for the animal cap assay. *Pitx1* mRNA (100 pg) was injected into the animal pole at the 4-cell stage. Animal caps were dissected at stage 8 and cultured to stage 16. (**J**) *Shroom3* and *Shroom1* expression levels in whole embryos, control caps, and *Pitx1*-injected caps were analyzed by RT-PCR using *Xag1* as a positive control and *Ef1α* as a loading control. *Shroom3* expression is induced following Pitx1 expression. (**K**) *Shroom3* expression is induced following Pitx3 expression in animal caps.

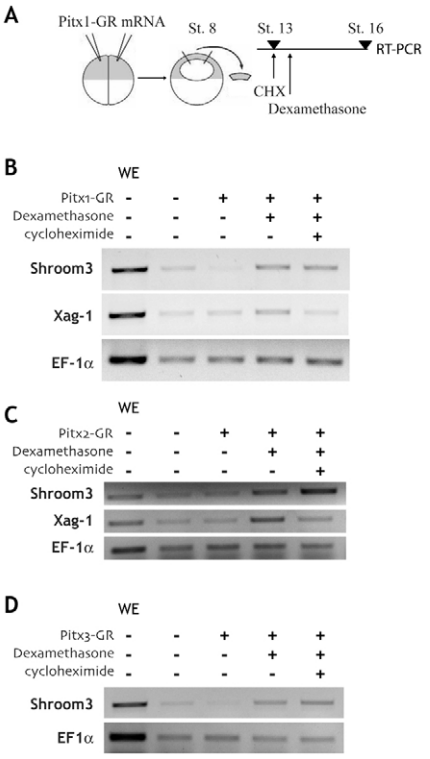

Fig. 7. Pitx1 directly activates *Shroom3* transcription. (**A**) Experimental scheme. *Pitx1-GR* mRNA was injected into the animal pole at the 4-cell stage. Animal caps were dissected at stage 8 and cultured. At stage 13, caps were first treated with cycloheximide (CHX) for 10 minutes and then treated with dexamethasone (DEX) and cultured to stage 16. (**B**) *Shroom3* and *Xag1* expression are induced by active Pitx1. *Shroom3* is consistently induced in the presence of both CHX and DEX, although *Xag1* is not activated by DEX in the presence of CHX. (**C**,**D**) The same experiment described in A, but using (C) *Pitx2-GR* and (D) *Pitx3-GR* mRNA. Similar data were obtained as for *Pitx1-GR*.

using targeted microinjection of *Pitx1* mRNA. Consistent with our hypothesis, mosaic Pitx1-expressing embryos displayed ectopic *Shroom3* expression in the epidermis (Fig. 6C,D). Similar results were obtained with Pitx2 and Pitx3 (Fig. 6E-H and data not shown). Moreover, ectopic Pitx expression in the epidermis resulted in ectopic pigment accumulation (Fig. 6B,F), a phenotype that is similar to that caused by ectopic expression of Shroom3 (Fairbank et al., 2006; Haigo et al., 2003) (see below).

We next confirmed these data by ectopically expressing Pitx1 in the pluripotent cells of early *Xenopus* embryos – the so-called animal cap. We injected *Pitx1* mRNA into the animal pole of early cleavage-stage embryos, and animal cap explants were removed at late blastula stages and cultured in vitro until mid-neurulation (Fig. 6I). RT-PCR revealed that *Shroom3* transcription was strongly induced by Pitx1 expression in these isolated cells (Fig. 6J). As a positive control for Pitx1 action, the expression of *Xag1*, a known downstream gene of Pitx1, was induced (Schweickert et al., 2001). By contrast, *Shroom1*, another Shroom family gene (Hagens et al., 2006), was not induced by ectopic Pitx1 (Fig. 6J). Similar results were also obtained with Pitx2 and Pitx3 (Fig. 6K; data not shown).

To ensure that this result was not specific to animal cap cells, we injected *Pitx1* mRNA into the vegetal blastomeres at the 8-cell stage. These cells give rise to endoderm and after culturing to gastrula stages, RT-PCR on the injected embryos revealed the activation of *Shroom3* expression (see Fig. S3 in the supplementary material). Pitx-expressing vegetal blastomeres explanted and cultured in isolation until tailbud stages also displayed activation of *Shroom3* transcription (not shown). Together, these data indicate that Pitx transcription factors are sufficient to drive Shroom3 expression. We therefore conclude that Shroom3 acts downstream of Pitx1 to control gut morphogenesis.

Pitx1 directly activates *Shroom3* transcription

To assess whether *Shroom3* is a direct target of Pitx1, we asked whether *Shroom3* transcription could still be activated by Pitx1 in the absence of protein synthesis. For this experiment, we precisely controlled the onset of Pitx1 activity using glucocorticoid-activatable Pitx constructs (Pitx-GR). The Pitx-GR fusion protein remains in the cytoplasm, and thus inactive, until addition of dexamethasone (DEX) allows it to translocate into the nucleus (Gammill and Sive, 1997; Kolm and Sive, 1995). The mRNA

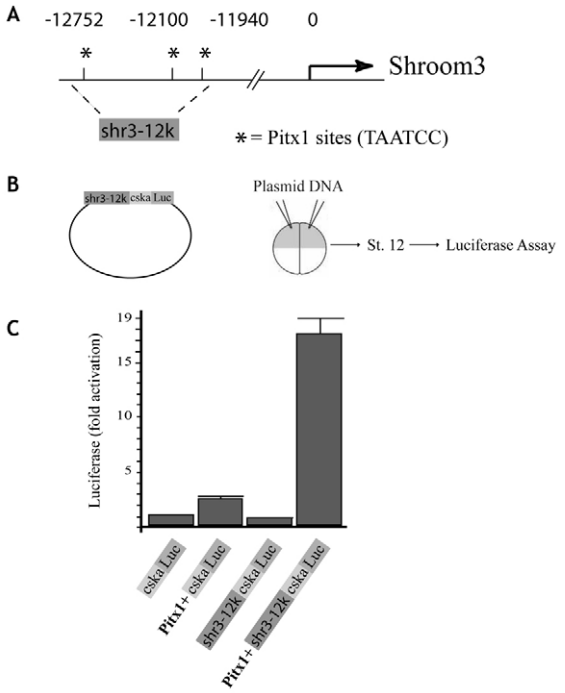

Fig. 8. A Pitx1-responsive enhancer is located 12 kb upstream of the *Shroom3* transcription start site. (**A**) Three Pitx1 consensus binding sites are located in a cluster ~12 kb upstream of the *Xenopus Shroom3* transcription start site. (**B**) The fragment containing these three sites (shr3-12k) was cloned into the pGL3-*Cska* minimal promoter-luciferase vector. Embryos at the 4-cell stage were injected in each blastomere with luciferase reporter constructs and *Pitx1* mRNA, as indicated in C. Embryos were collected at stage 12 for luciferase assays. (**C**) Normalized luciferase activity. Together with Pitx1 expression, inclusion of the shr3-12k region increases luciferase activity ~18-fold above the basal level observed with the minimal promoter alone.

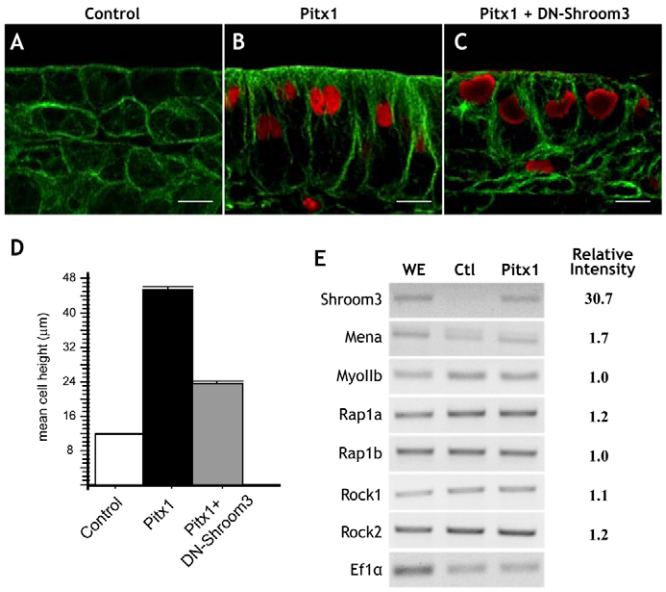

Fig. 9. Ectopic Pitx1 expression induces epithelial cell shape change and the assembly of parallel microtubule arrays. (**A**) Control epidermis cells. α-tubulin staining reveals cell cortices. (**B**) Epidermis cells expressing ectopic Pitx1 are marked by His2B-GFP (red nuclei) and are stained for α-tubulin. Cells expressing Pitx1 apically constrict and elongate 4-fold (~45 μm; *n*=32) as compared with control cells (~11 μm; *n*=20). This difference is extremely significant (*P*<0.0001; Mann-Whitney U-test). Robust MT arrays emanate from the apical cell surface. (**C**) Epidermis cells expressing ectopic Pitx1 and DN-Shroom3 are marked by His2B-GFP (red nuclei) and are stained for α-tubulin. Apical constriction and apicobasal elongation revert to ~24 μm for Pitx1 + DN-Shroom3 (*n*=29; *P*<0.0001). MT bundles observed in Pitx1-expressing cells are also eliminated following DN-Shroom3 expression. Scale bars: 10 μm. (**D**) The apicobasal cell height of control, Pitx1-expressing, and Pitx1 + DN-Shroom3-expressing epidermis cells. (**E**) RT-PCR analysis of the expression of Shroom3 effectors in animal cap assays. *Shroom3* expression was induced ~30-fold following Pitx1 expression. A modest increase in *Mena* expression (~1.7-fold) was observed, whereas *MyoIIb*, *Rap1a/b* and *Rock1/2* genes were unaffected. *Ef1α* provided a loading control.

encoding Pitx1-GR was injected and animal caps dissected as described above. However, in this experiment, animal caps were first incubated with cycloheximide (CHX) to block translation and only later treated with DEX to activate Pitx1-GR (Fig. 7A). Using RT-PCR, we observed that transcription of *Shroom3* and *Xag1* was clearly induced by active Pitx1-GR, but not by the inactive Pitx1-GR in the absence of DEX (Fig. 7B, lanes 3 and 4). Moreover, expression of *Shroom3* was consistently induced in the presence of both DEX and CHX, indicating that it was a direct target of Pitx1 (Fig. 7B, lane 5). By contrast, *Xag1* was not induced by DEX in the presence of CHX (Fig. 7B, lane 5). Similar data were obtained with Pitx2-GR and Pitx3-GR (Fig. 7C,D).

If *Shroom3* is a direct target of Pitx transcription factors, then we would expect to find Pitx consensus binding sites in the vicinity of the *Shroom3* gene. We found many imperfect Pitx sites near the *Shroom3* transcription start site in the *Xenopus tropicalis* genome, but three ideal Pitx consensus binding sites [TAAT/GCC (Lamonerie et al., 1996)] ~12 kb upstream of the *Shroom3* transcription start (Fig. 8A). The genomic DNA from the putative regulatory region containing these sites (shr3-12k) was placed upstream of a minimal promoter driving luciferase, and a plasmid containing this reporter construct was then injected into embryos that were cultured and then analyzed for luciferase activity (Fig. 8B). The shr3-12k construct drove only very modest expression of luciferase in control embryos. However, expression of Pitx1 by mRNA injection increased luciferase activity ~18-fold above the basal level observed with the minimal promoter only (Fig. 8C). Together, these data suggest that Pitx transcription factors directly activate *Shroom3* transcription.

Ectopic Pitx1 induces epithelial cell shape change and assembly of parallel microtubule arrays

Shroom3 is sufficient to drive epithelial cell shape change (Haigo et al., 2003; Lee et al., 2007). If Pitx factors induce Shroom3 expression, then we would predict that ectopic Pitx1 would induce similar changes in cell shape. Again, we used targeted microinjection of *Pitx1* mRNA to generate mosaic epidermis in which a subset of cells express ectopic Pitx1; we then compared cell morphology in Pitx1-expressing cells to that of neighboring, non-expressing cells. To trace cells expressing ectopic Pitx1, mRNA encoding histone H2B linked to GFP (His2B-GFP) was co-injected. We found that Pitx1-expressing epithelial cells apically constricted and elongated dramatically compared with neighboring

cells that lacked Pitx1 expression (Fig. 9A,B). Ectopic Pitx1 drove epithelial cells to elongate 4-fold compared with control cells (Fig. 9D).

Shroom3-mediated cell elongation acts via γ-tubulin accumulation and MT assembly (Lee et al., 2007). Noticeably, robust MT arrays emanating from the apical surface were consistently observed in Pitx1-expressing cells, but not control cells (Fig. 9A,B). Similar results were obtained with ectopic expression of Pitx2 or Pitx3 (see Fig. S4B,E in the supplementary material). Likewise, ectopic Pitx expression resulted in an increase in cytoplasmic γ-tubulin signal in epidermal epithelial cells (see Fig. S5 in the supplementary material). Localization of ZO-1 in epidermal cells was unaffected by ectopic Pitx expression (not shown). Together, these data demonstrate that ectopic Pitx expression can drive the assembly of MT arrays and induce epithelial cell shape changes similar to those observed following ectopic Shroom3 expression in epithelial cells.

Pitx1-induced changes in cell behavior are Shroom3 dependent

Next, we asked whether these Pitx1-induced epithelial cell shape changes depend upon Shroom3 by generating mosaic embryos containing cells that co-express Pitx1 and DN-Shrm3. Following co-expression of DN-Shrm3, the Pitx1-induced apicobasal elongation was reduced by more than half (Fig. 9C,D). Moreover, DN-Shrm3 in the neural tube disrupts the assembly of parallel MTs (Lee et al., 2007), and we found that the apical MT bundles and excess γ-tubulin signal induced in epithelial cells by ectopic Pitx1 were almost entirely eliminated by co-expression of DN-Shrm3 (Fig. 9C; see Fig. S5 in the supplementary material). Similar results were obtained when DN-Shrm3 was co-expressed with Pitx2 or Pitx3 (see Fig. S4C,F in the supplementary material). Together, these data indicate that Pitx1 controls epithelial cell shape changes via a Shroom3-dependent mechanism.

Pitx1 does not robustly activate the expression of genes that encode known Shroom3 effector proteins

Shroom3 has been shown to control epithelial cell shape changes by working in concert with several effector proteins, including myosin II, Mena, Rap1 and Rho kinase (Haigo et al., 2003; Hildebrand, 2005; Hildebrand and Soriano, 1999; Nishimura and Takeichi, 2008). We therefore monitored expression in pluripotent cells to examine whether Pitx1 also controls the transcription of the genes that encode these proteins. In this assay, *Shroom3* transcription was increased ~30-fold following Pitx1 expression (Fig. 9E). By contrast, *Mena* showed only a very modest (~1.7-fold) increase in expression levels following Pitx1 expression, and the transcriptional levels of *MyoIIb*, *Rap1a*, *Rap1b*, *Rock1* and *Rock2* were unaffected (Fig. 9E). Similar results were obtained with Pitx2 and Pitx3 (see Fig. S4G,H in the supplementary material). However, two caveats must be borne in mind here. First, it is possible that the baseline transcription of these effectors in animal cap cells masks some level of activation by Pitx factors. We consider this unlikely, as Xag1 is also expressed in animal caps and we were able to detect clear elevation of *Xag1* transcription following Pitx expression (Fig. 6J). Second, it is important to note that our results do not exclude a role for these genes in cell shape changes, as post-translational regulation of these effectors is key to their activity.

These data are consistent with our previous findings that increased levels of Shroom3 alone are sufficient to drive cell shape change in multiple epithelial cell types (Haigo et al., 2003; Hildebrand, 2005). Moreover, the results reveal a straightforward genetic program whereby Pitx1 directly activates *Shroom3*, which is sufficient to initiate the thickening and bending of epithelial sheets.

DISCUSSION

Epithelial cell shape changes contribute significantly to morphogenesis in most metazoan animals. Nonetheless, the developmental control of such shape changes has been studied predominantly in only a small number of tissues, such as the vertebrate neural plate and the ventral furrow and salivary glands of *Drosophila* (Leptin and Grunewald, 1990; Myat and Andrew, 2002; Schoenwolf, 1988). Shroom3 has emerged as a major player in the developmental regulation of epithelial cell shape changes in vertebrates (Haigo et al., 2003; Hildebrand, 2005; Lee et al., 2007; Nishimura and Takeichi, 2008). Here, we have addressed two key unanswered questions in this field.

First, despite widespread expression (Hildebrand and Soriano, 1999; Lee et al., 2009), Shroom3 function has never been explored by loss-of-function approaches outside the neural epithelium. We show here for the first time that Shroom3 is required for morphogenesis of endodermal tissues. We show that Shroom3 governs cell shape and morphogenesis in the archenteron epithelium and also in the more mature gut epithelium (Fig. 1).

Second, little is known about the transcriptional control of cell shape change in vertebrate epithelia. We identify here the first known transcriptional regulator of Shroom3 by showing that Pitx proteins are necessary and sufficient to directly activate *Shroom3* transcription (Figs 4-8). Indeed, disruption of Pitx1 phenocopies disruption of Shroom3 in the gut (Figs 2, 4). These results are important, as they shed light on the general problem of transcriptional control of epithelial morphogenesis. The results are also meaningful because Pitx expression has been correlated with epithelial cell shape change, but no Pitx targets had previously been identified that could explain this correlation (Davis et al., 2008; Rodriguez-Leon et al., 2008). We show that Pitx transcription factors are sufficient to induce epithelial cell shape changes via activation of *Shroom3* in naïve cells (Fig. 9), suggesting that regulation of *Shroom3* transcription might be a general mechanism by which Pitx factors drive morphogenesis. Thus, our data provide key insights into gut morphogenesis, the transcriptional regulation of epithelial cell shape, and the mode of action of the Pitx family of transcription factors.

The role of Shroom3 in gut morphogenesis

We have shown here that Shroom3 is essential for the morphogenesis of the *Xenopus* gut. We find that cells lacking Shroom3 (or Pitx1) fail to elongate along the apicobasal axis, both in the archenteron floor and later in the mature gut. In *Xenopus*, gut elongation is achieved in part by the radial intercalation of elongated endodermal cells into a single layer (Chalmers and Slack, 2000; Reed et al., 2009), and changes in the thickness of the gut epithelium then help to drive the subsequent morphogenesis of the gut tube (Chalmers and Slack, 1998; Muller et al., 2003; Reed et al., 2009). Our data linking Shroom3 with cell elongation and gut morphogenesis (Figs 1, 2) are thus consistent with the current models for *Xenopus* gut development.

Recent papers have sought to address the mechanisms by which such morphogenetic events are influenced by regionally restricted signaling events in the gut. For example, it has been shown that cell intercalations controlled by non-canonical Wnt [planar cell polarity (PCP)] signaling act specifically in the *Xenopus* hindgut, where Cdx

genes activate the expression of Wnt genes to effect gut morphogenesis (Faas and Isaacs, 2009; Li et al., 2008). In these posterior endodermal tissues, morphogenesis is driven largely by convergent extension cell rearrangements (Chalmers and Slack, 2000; Horb and Slack, 2001; Larkin and Danilchik, 1999). These PCP-dependent processes are normally repressed in the anterior gut by expression of the secreted Wnt antagonist Sfrp (Li et al., 2008; Matsuyama et al., 2009), so additional morphogenetic motors must be at work in this tissue. Thus, it is possible that Shroom3-mediated cell shape changes play a more important role in the rostral gut, as compared with the caudal gut. Indeed, there is evidence to suggest a possible link between Shroom3 and Sfrp. Sfrp is required for the integrity of the foregut epithelium in both mice and frogs (Li et al., 2008; Matsuyama et al., 2009), and we found that disruption of Shroom3 function resulted in a failure of the integrity of the gut epithelium (Fig. 1).

The possibility that Shroom3 plays an especially important role in the anterior gut, whereas PCP signaling acts more posteriorly, is intriguing, as a parallel situation has been delineated in the developing vertebrate neural tube. In both *Xenopus* and mice, Shroom3-mediated cell shape changes are essential for anterior neural tube closure, but play a less crucial role in posterior neural tube closure (Haigo et al., 2003; Hildebrand and Soriano, 1999); conversely, PCP-mediated cell rearrangements are required for posterior, but not anterior, neural tube morphogenesis (see Wallingford, 2005).

Finally, when considering gut morphogenesis, one must address not only the complexity of gut lengthening, but also the left-right asymmetric morphogenesis of this organ. Pitx2 is a major player in asymmetric left-right morphogenesis of the gut (Capdevila et al., 2000; Logan et al., 1998) and, indeed, ectopic expression of Pitx2 can drive the formation of ectopic concavities in the *Xenopus* gut (Muller et al., 2003). However, the molecular and cellular bases of Pitx action during morphogenesis remain unknown. Given that gut looping in *Xenopus* is likely to be driven by cell shape changes in the gut epithelium itself (Muller et al., 2003) and that Pitx2 can directly activate *Shroom3* expression (Fig. 7), our data suggest that Pitx2 induction of Shroom3-mediated cell shape changes might drive chiral gut looping in *Xenopus*. It is worth noting that this mechanism might be conserved to some degree in mice, in which gut looping is directed by Pitx2-controlled apicobasal cell elongation in the dorsal mesentery (Davis et al., 2008). These results are made even more tantalizing by the fact that there are Pitx binding sites upstream of mouse *Shroom3*, and both *Pitx2* and *Shroom3* mutant mice display a similar gastroschisis phenotype (Hildebrand and Soriano, 1999; Kitamura et al., 1999). Clearly, additional experiments will be required, but our present data suggest that Shroom3, under the control of Pitx transcription factors, plays a central role in the morphogenesis of the vertebrate gut.

Transcriptional programs that are sufficient to initiate epithelial morphogenesis

Tissue morphogenesis occurs via the developmentally regulated control of individual cell behaviors (Holtfreter, 1943; Trinkaus, 1969). Thus, any comprehensive picture of the molecular basis of morphogenesis will require an understanding of how genes that control embryo patterning (e.g. transcription factors) affect the cytoskeletal and adhesion components that ultimately drive cell behaviors. Recent progress has been made in this area through genome-wide screens for genes that are differentially expressed in migrating cell populations (Borghese et al., 2006; Christiaen et al., 2008; Wang et al., 2006). These studies have revealed that large numbers of genes encoding cytoskeletal proteins are transcriptionally regulated during migration. Epithelial sheet thickening and bending are comparatively simple, although equally essential, morphogenetic processes, and our data suggest that surprisingly simple transcriptional programs might be sufficient to initiate them.

Our data suggest that a fairly direct transcriptional route is sufficient to initiate epithelial sheet thickening and bending in *Xenopus*, as we find that Pitx transcription factors directly activate the transcription of *Shroom3*. Additional evidence that this simple genetic system is sufficient comes from the ability of Pitx transcription factors to drive Shroom3-mediated cell shape changes without activating the transcription of known Shroom3 effectors, including Mena, myosin II, Rho kinases and Rap1 GTPases (Haigo et al., 2003; Hildebrand, 2005; Hildebrand and Soriano, 1999; Nishimura and Takeichi, 2008). It should be noted, however, that disruption of Shroom3 failed to entirely suppress Pitx-induced cell shape changes (Fig. 9A-D). This result might suggest that other, as yet unidentified, Pitx targets contribute to cell shape changes, or the result might simply reflect a limitation in the experimental approach (higher doses of DN-Shrm3 in this context caused cell death and thus could not be tested).

The apparent simplicity of this sufficient program relies on the remarkable ability of Shroom3 to reorganize cytoskeletal systems specifically in epithelial cells. Shroom3 alone is sufficient to drive actin/myosin-based apical constriction and γ-tubulin/MT-based cell elongation (Haigo et al., 2003; Hildebrand, 2005; Lee et al., 2007). This program is specific to polarized epithelial cells, as expression of Shroom3 in mesenchymal cells has no effect. Moreover, Shroom3 can drive these changes in the epithelial cells of *Xenopus* blastulae, where transcription is strongly suppressed by a variety of mechanisms (Haigo et al., 2003; Newport and Kirschner, 1982; Stancheva et al., 2002). Thus, both actin- and MT-based cell shape changes induced by Shroom3 are organized in the absence of nascent transcription. If Shroom3-mediated changes in cell behavior do not require nascent transcription, then transcriptional control of *Shroom3* itself must be a key node for patterning epithelial morphogenesis in vertebrates. The present work demonstrates that the Pitx family of transcription factors plays a central role by directly activating *Shroom3* transcription (Figs 6, 7).

The model that emerges from this work has interesting parallels in invertebrate systems. Indeed, although *Drosophila* does not appear to use a Shroom family protein for epithelial folding, a similarly straightforward system is nonetheless sufficient to initiate epithelial morphogenesis. As with vertebrate Shroom3, the ectopic expression of a single *Drosophila* protein, Folded gastrulation (Fog), is sufficient to drive apical constriction (Morize et al., 1998). Moreover, a downstream effector of Fog, RhoGEF2, is also sufficient by itself to drive apical constriction and cell elongation when ectopically expressed (Barrett et al., 1997; Hacker and Perrimon, 1998; Nikolaidou and Barrett, 2004; Rogers et al., 2004). A simple transcriptional system appears to be employed here as well, as the transcription factor Twist is essential for *fog* expression and ChIP-on-chip experiments suggest that *fog* is a direct target of Twist (Morize et al., 1998; Zeitlinger et al., 2007). As noted above, Pitx factors might activate the expression of as yet unidentified effectors, and a candidate might be a vertebrate protein that is functionally analogous to T48, which is a direct target of Twist that is involved in apical constriction during *Drosophila* gastrulation (Kolsch et al., 2007). Regardless, in both *Drosophila* and *Xenopus*, a simple and sufficient system can be delineated that involves a single transcription factor (Twist/Pitx) that directly activates the expression of a protein that is sufficient to drive apical constriction (Fog/Shroom3).

Conclusions

Our data linking a transcriptional regulator directly to a cytoskeletal regulator reveal a minimally sufficient system for initiating epithelial cell shape changes in vertebrate morphogenesis. Although the proteins involved are not shared, the system has striking parallels to that in *Drosophila*. We show that this Pitx1→Shroom3 system is crucial for gut morphogenesis in *Xenopus*. It should be noted that this system is likely to play a far broader role in cell shape and morphogenesis, as Shroom3 is also required for morphogenesis of the lens (Plageman et al., 2010), where Pitx proteins are expressed (Gage et al., 1999b; Pommereit et al., 2001; Schweickert et al., 2001). Much work remains to be done, however, as no known Pitx transcription factors are expressed at the right time and place to explain the expression of Shroom3 in the neural tube, where it is essential for closure (Haigo et al., 2003). Indeed, given the complexity of transcriptional regulation during development, it is very likely that the control of Shroom3 expression in vivo requires a myriad of additional transcriptional inputs, even in the gut. Nonetheless, the simplicity of this sufficient system is intriguing, and might be of use in tissue engineering approaches (e.g. Davies, 2008). Our data provide important new insights into the transcriptional networks that control epithelial cell shape change in developing vertebrate embryos. Given the widespread expression of Shroom3 in epithelial tissues, and the essential role for Shroom3 in morphogenesis, elucidating such networks will be crucial for a comprehensive understanding of vertebrate tissue morphogenesis.

Acknowledgements

We thank T. J. Plageman, Richard Lang, Steve Vokes and Chanjae Lee for important insights into this project; Andy Ewald, Sara Peyrot and Katherine Smith for critical reading of the manuscript; and Heather Scherr for technical help. This work was supported by grants from the NSF (IOB 0642012) to N.M.N.; the Canadian Institutes of Health Research (MOP-74663) to T.A.D.; the NIH/NIGMS, The March of Dimes, and the Burroughs Wellcome Fund to J.B.W. J.B.W. is an Early Career Scientist of the Howard Hughes Medical Institute. Deposited in PMC for release after 6 months.

Competing interests statement

The authors declare no competing financial interests.

Supplementary material

Supplementary material for this article is available at
http://dev.biologists.org/lookup/suppl/doi:10.1242/dev.044610/-/DC1

References

Barrett, K., Leptin, M. and Settleman, J. (1997). The Rho GTPase and a putative RhoGEF mediate a signaling pathway for the cell shape changes in Drosophila gastrulation. *Cell* **91**, 905-915.

Borghese, L., Fletcher, G., Mathieu, J., Atzberger, A., Eades, W. C., Cagan, R. L. and Rorth, P. (2006). Systematic analysis of the transcriptional switch inducing migration of border cells. *Dev. Cell* **10**, 497-508.

Burnside, B. (1973). Microtubules and microfilaments in amphibian neurulation. *Amer. Zool.* **13**, 989-1006.

Burnside, M. B. and Jacobson, A. G. (1968). Analysis of morphogenetic movements in the neural plate of the newt Taricha torosa. *Dev. Biol.* **18**, 537-552.

Capdevila, J., Vogan, K. J., Tabin, C. J. and Izpisua Belmonte, J. C. (2000). Mechanisms of left-right determination in vertebrates. *Cell* **101**, 9-21.

Chalmers, A. D. and Slack, J. M. (1998). Development of the gut in Xenopus laevis. *Dev. Dyn.* **212**, 509-521.

Chalmers, A. D. and Slack, J. M. (2000). The Xenopus tadpole gut: fate maps and morphogenetic movements. *Development* **127**, 381-392.

Christiaen, L., Davidson, B., Kawashima, T., Powell, W., Nolla, H., Vranizan, K. and Levine, M. (2008). The transcription/migration interface in heart precursors of Ciona intestinalis. *Science* **320**, 1349-1352.

Davidson, L. A. and Wallingford, J. B. (2005). Visualizing cell biology and tissue movements during morphogenesis in the frog embryo. In *Imaging in Neuroscience and Development* (ed. R. Yuste and A. Konnerth), pp. 125-136. Cold Spring Harbor, New York: Cold Spring Harbor Laboratory Press.

Davies, J. A. (2008). Synthetic morphology: prospects for engineered, self-constructing anatomies. *J. Anat.* **212**, 707-719.

Davis, N. M., Kurpios, N. A., Sun, X., Gros, J., Martin, J. F. and Tabin, C. J. (2008). The chirality of gut rotation derives from left-right asymmetric changes in the architecture of the dorsal mesentery. *Dev. Cell* **15**, 134-145.

Faas, L. and Isaacs, H. V. (2009). Overlapping functions of Cdx1, Cdx2, and Cdx4 in the development of the amphibian Xenopus tropicalis. *Dev. Dyn.* **238**, 835-852.

Fairbank, P. D., Lee, C., Ellis, A., Hildebrand, J. D., Gross, J. M. and Wallingford, J. B. (2006). Shroom2 (APXL) regulates melanosome biogenesis and localization in the retinal pigment epithelium. *Development* **133**, 4109-4118.

Gage, P. J., Suh, H. and Camper, S. A. (1999a). Dosage requirement of Pitx2 for development of multiple organs. *Development* **126**, 4643-4651.

Gage, P. J., Suh, H. and Camper, S. A. (1999b). The bicoid-related Pitx gene family in development. *Mamm. Genome* **10**, 197-200.

Gammill, L. S. and Sive, H. (1997). Identification of otx2 target genes and restrictions in ectodermal competence during Xenopus cement gland formation. *Development* **124**, 471-481.

Hacker, U. and Perrimon, N. (1998). DRhoGEF2 encodes a member of the Dbl family of oncogenes and controls cell shape changes during gastrulation in Drosophila. *Genes Dev.* **12**, 274-284.

Hagens, O., Ballabio, A., Kalscheuer, V., Kraehenbuhl, J. P., Schiaffino, M. V., Smith, P. R., Staub, O., Hildebrand, J. and Wallingford, J. B. (2006). A new standard nomenclature for proteins related to Apx and Shroom. *BMC Cell Biol.* **7**, 18.

Haigo, S. L., Hildebrand, J. D., Harland, R. M. and Wallingford, J. B. (2003). Shroom induces apical constriction and is required for hingepoint formation during neural tube closure. *Curr. Biol.* **13**, 2125-2137.

Hildebrand, J. D. (2005). Shroom regulates epithelial cell shape via the apical positioning of an actomyosin network. *J. Cell Sci.* **118**, 5191-5203.

Hildebrand, J. D. and Soriano, P. (1999). Shroom, a PDZ domain-containing actin-binding protein, is required for neural tube morphogenesis in mice. *Cell* **99**, 485-497.

Holtfreter, J. (1943). A study of the mechanics of gastrulation, part I. *J. Exp. Zool.* **94**, 261-318.

Horb, M. E. and Slack, J. M. (2001). Endoderm specification and differentiation in Xenopus embryos. *Dev. Biol.* **236**, 330-343.

Jacobson, A. G. and Gordon, R. (1976). Changes in the shape of the developing vertebrate nervous system analyzed experimentally, mathematically and by computer simulation. *J. Exp. Zool.* **197**, 191-246.

Kitamura, K., Miura, H., Miyagawa-Tomita, S., Yanazawa, M., Katoh-Fukui, Y., Suzuki, R., Ohuchi, H., Suehiro, A., Motegi, Y., Nakahara, Y. et al. (1999). Mouse Pitx2 deficiency leads to anomalies of the ventral body wall, heart, extra- and periocular mesoderm and right pulmonary isomerism. *Development* **126**, 5749-5758.

Kolm, P. J. and Sive, H. L. (1995). Efficient hormone-inducible protein function in Xenopus laevis. *Dev. Biol.* **171**, 267-272.

Kolsch, V., Seher, T., Fernandez-Ballester, G. J., Serrano, L. and Leptin, M. (2007). Control of Drosophila gastrulation by apical localization of adherens junctions and RhoGEF2. *Science* **315**, 384-386.

Lamonerie, T., Tremblay, J. J., Lanctot, C., Therrien, M., Gauthier, Y. and Drouin, J. (1996). Ptx1, a bicoid-related homeo box transcription factor involved in transcription of the pro-opiomelanocortin gene. *Genes Dev.* **10**, 1284-1295.

Larkin, K. and Danilchik, M. V. (1999). Ventral cell rearrangements contribute to anterior-posterior axis lengthening between neurula and tailbud stages in Xenopus laevis. *Dev. Biol.* **216**, 550-560.

Lee, C., Scherr, H. M. and Wallingford, J. B. (2007). Shroom family proteins regulate gamma-tubulin distribution and microtubule architecture during epithelial cell shape change. *Development* **134**, 1431-1441.

Lee, C., Gray, R. S., Park, T. J. and Wallingford, J. B. (2008). Whole-mount fluorescence immunocytochemistry on Xenopus embryos. *Cold Spring Harb. Protoc.* doi:10.1101/pdb.prot4957.

Lee, C., Le, M. P. and Wallingford, J. B. (2009). The shroom family proteins play broad roles in the morphogenesis of thickened epithelial sheets. *Dev. Dyn.* **238**, 1480-1491.

Leptin, M. and Grunewald, B. (1990). Cell shape changes during gastrulation in Drosophila. *Development* **110**, 73-84.

Li, Y., Rankin, S. A., Sinner, D., Kenny, A. P., Krieg, P. A. and Zorn, A. M. (2008). Sfrp5 coordinates foregut specification and morphogenesis by antagonizing both canonical and noncanonical Wnt11 signaling. *Genes Dev.* **22**, 3050-3063.

Logan, M., Pagan-Westphal, S. M., Smith, D. M., Paganessi, L. and Tabin, C. J. (1998). The transcription factor Pitx2 mediates situs-specific morphogenesis in response to left-right asymmetric signals. *Cell* **94**, 307-317.

Matsuyama, M., Aizawa, S. and Shimono, A. (2009). Sfrp controls apicobasal polarity and oriented cell division in developing gut epithelium. *PLoS Genet.* **5**, e1000427.

Moody, S. A. and Kline, M. J. (1990). Segregation of fate during cleavage of frog (Xenopus laevis) blastomeres. *Anat. Embryol.* **182**, 347-362.

Morize, P., Christiansen, A. E., Costa, M., Parks, S. and Wieschaus, E. (1998). Hyperactivation of the folded gastrulation pathway induces specific cell shape changes. *Development* **125**, 589-597.
Muller, J. K., Prather, D. R. and Nascone-Yoder, N. M. (2003). Left-right asymmetric morphogenesis in the Xenopus digestive system. *Dev. Dyn.* **228**, 672-682.
Myat, M. M. and Andrew, D. J. (2002). Epithelial tube morphology is determined by the polarized growth and delivery of apical membrane. *Cell* **111**, 879-891.
Newport, J. and Kirschner, M. (1982). A major developmental transition in early Xenopus embryos: II. Control of the onset of transcription. *Cell* **30**, 687-696.
Nieuwkoop, P. D. and Faber, J. (1967). *Normal Table of Xenopus laevis.* New York: Garland.
Nikolaidou, K. K. and Barrett, K. (2004). A Rho GTPase signaling pathway is used reiteratively in epithelial folding and potentially selects the outcome of Rho activation. *Curr. Biol.* **14**, 1822-1826.
Nishimura, T. and Takeichi, M. (2008). Shroom3-mediated recruitment of Rho kinases to the apical cell junctions regulates epithelial and neuroepithelial planar remodeling. *Development* **135**, 1493-1502.
Plageman, T., Chung, M., Lou, M., Smith, A., Hildebrand, J., Wallingford, J. and Lang, R. (2010). Pax6-dependent Shroom3 expression regulates apical constriction during lens placode invagination. *Development* **137**, 405-415.
Pommereit, D., Pieler, T. and Hollemann, T. (2001). Xpitx3: a member of the Rieg/Pitx gene family expressed during pituitary and lens formation in Xenopus laevis. *Mech. Dev.* **102**, 255-257.
Reed, R. A., Womble, M. A., Dush, M. K., Tull, R. R., Bloom, S. K., Morckel, A. R., Devlin, E. W. and Nascone-Yoder, N. M. (2009). Morphogenesis of the primitive gut tube is generated by Rho/ROCK/myosin II-mediated endoderm rearrangements. *Dev. Dyn.* **238**, 3111-3125.
Rodriguez-Leon, J., Rodriguez Esteban, C., Marti, M., Santiago-Josefat, B., Dubova, I., Rubiralta, X. and Izpisua Belmonte, J. C. (2008). Pitx2 regulates gonad morphogenesis. *Proc. Natl. Acad. Sci. USA* **105**, 11242-11247.
Rogers, S. L., Wiedemann, U., Hacker, U., Turck, C. and Vale, R. D. (2004). Drosophila RhoGEF2 associates with microtubule plus ends in an EB1-dependent manner. *Curr. Biol.* **14**, 1827-1833.
Schoenwolf, G. C. (1988). Microsurgical analyses of avian neurulation: separation of medial and lateral tissues. *J. Comp. Neurol.* **276**, 498-507.
Schoenwolf, G. C. (1991). Cell movements driving neurulation in avian embryos. *Development* **Suppl. 2**, 157-168.
Schweickert, A., Steinbeisser, H. and Blum, M. (2001). Differential gene expression of Xenopus Pitx1, Pitx2b and Pitx2c during cement gland, stomodeum and pituitary development. *Mech. Dev.* **107**, 191-194.
Sive, H. L., Grainger, R. M. and Harland, R. M. (2000). *Early Development of Xenopus laevis*: *A Laboratory Manual.* Cold Spring Harbor, New York: Cold Spring Harbor Laboratory Press.
Stancheva, I., El-Maarri, O., Walter, J., Niveleau, A. and Meehan, R. R. (2002). DNA methylation at promoter regions regulates the timing of gene activation in Xenopus laevis embryos. *Dev. Biol.* **243**, 155-165.
Sweeton, D., Parks, S., Costa, M. and Wieschaus, E. (1991). Gastrulation in Drosophila: the formation of the ventral furrow and posterior midgut invaginations. *Development* **112**, 775-789.
Trinkaus, J. P. (1969). *Cell Into Organs – The Forces That Shape The Embryo*. Englewood Cliffs, New Jersey: Prentice-Hall.
Viamontes, G. I. and Kirk, D. L. (1977). Cell shape changes and the mechanism of inversion in Volvox. *J. Cell Biol.* **75**, 719-730.
Wallingford, J. B. (2005). Neural tube closure and neural tube defects: studies in animal models reveal known knowns and known unknowns. *Am. J. Med. Genet.* **135**, 59-68.
Wang, X., Bo, J., Bridges, T., Dugan, K. D., Pan, T. C., Chodosh, L. A. and Montell, D. J. (2006). Analysis of cell migration using whole-genome expression profiling of migratory cells in the Drosophila ovary. *Dev. Cell* **10**, 483-495.
Zeitlinger, J., Zinzen, R. P., Stark, A., Kellis, M., Zhang, H., Young, R. A. and Levine, M. (2007). Whole-genome ChIP-chip analysis of Dorsal, Twist, and Snail suggests integration of diverse patterning processes in the Drosophila embryo. *Genes Dev.* **21**, 385-390.

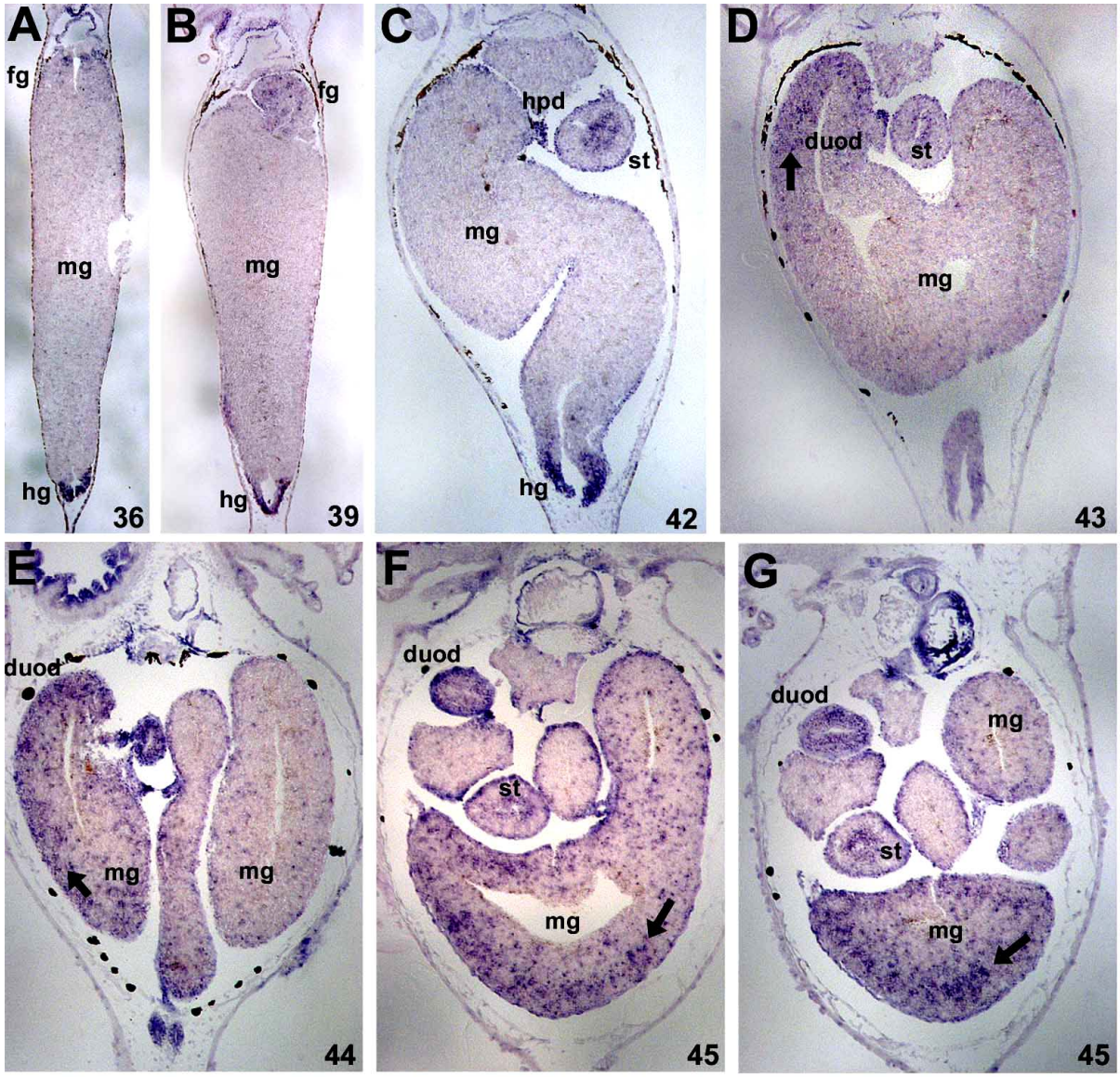
A
fg
mg
hg
36
B
fg
mg
hg
39
C
hpd
st
mg
hg
42
D
duod
st
mg
43
E
duod
mg
mg
44
F
duod
st
mg
45
G
duod
mg
st
mg
45

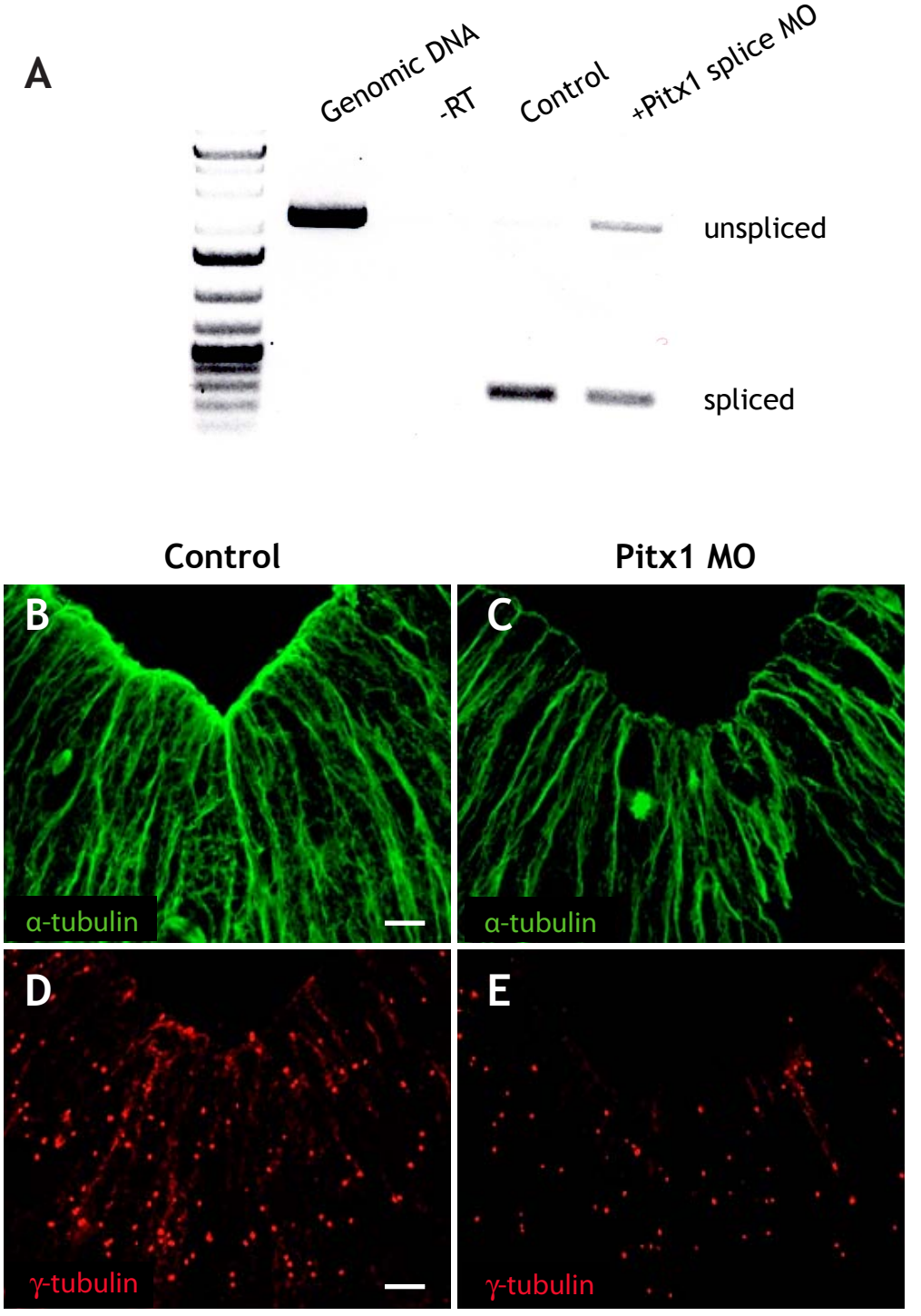
A
Genomic DNA
-RT
Control
+Pitx1 splice MO
unspliced
spliced
Control
Pitx1 MO
B
α-tubulin
C
α-tubulin
D
γ-tubulin
E
γ-tubulin

A

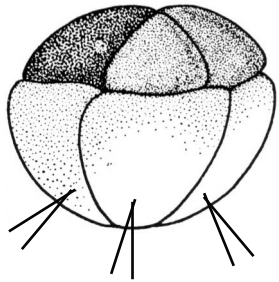

St. 10.5

Pitx1 mRNA

B

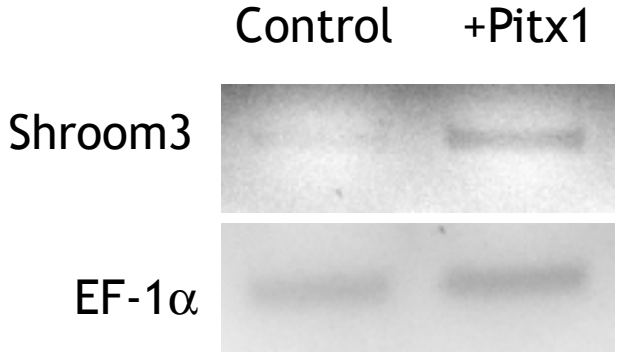

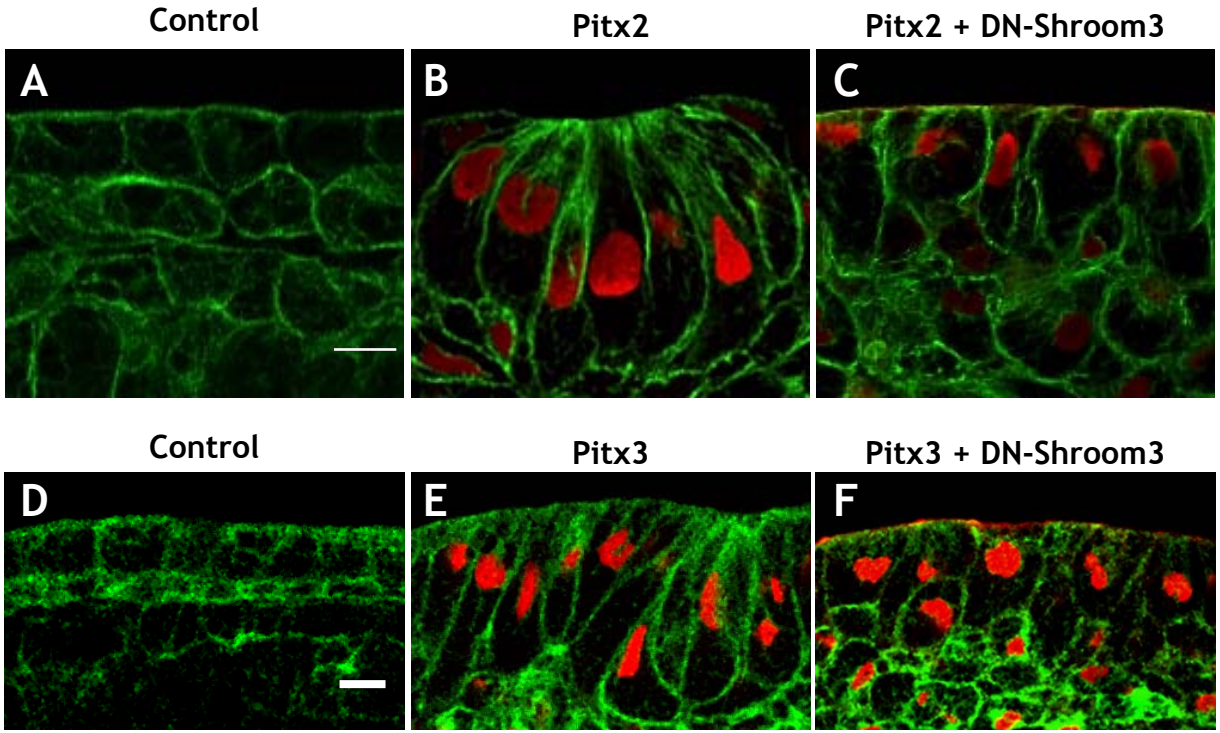
Control
Pitx2
Pitx2 + DN-Shroom3
A
B
C
Control
Pitx3
Pitx3 + DN-Shroom3
D
E
F

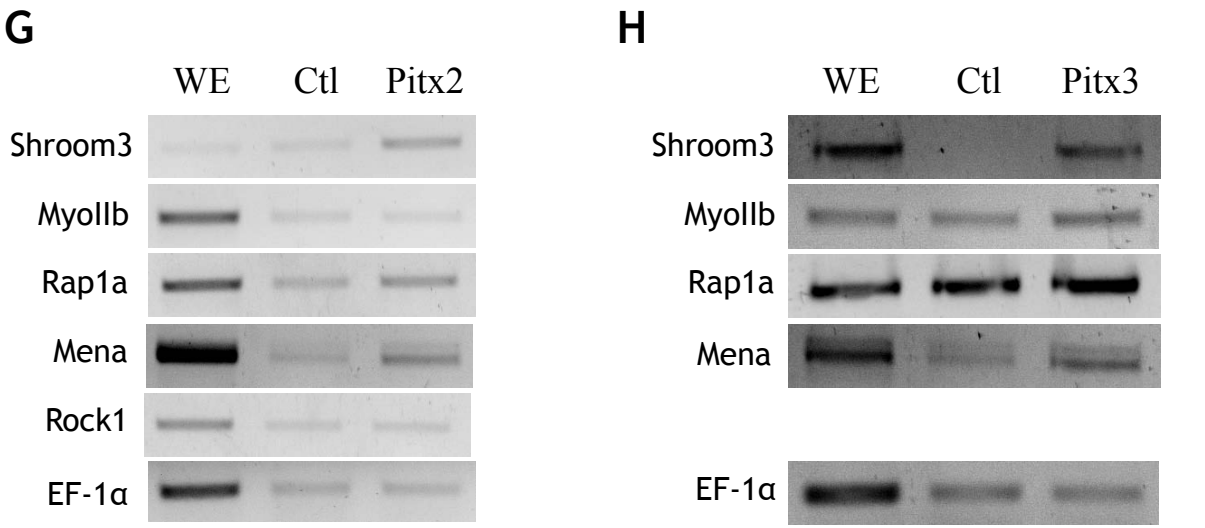
G
WE
Ctl
Pitx2
Shroom3
MyoIIb
Rap1a
Mena
Rock1
EF-1α
H
WE
Ctl
Pitx3
Shroom3
MyoIIb
Rap1a
Mena
EF-1α

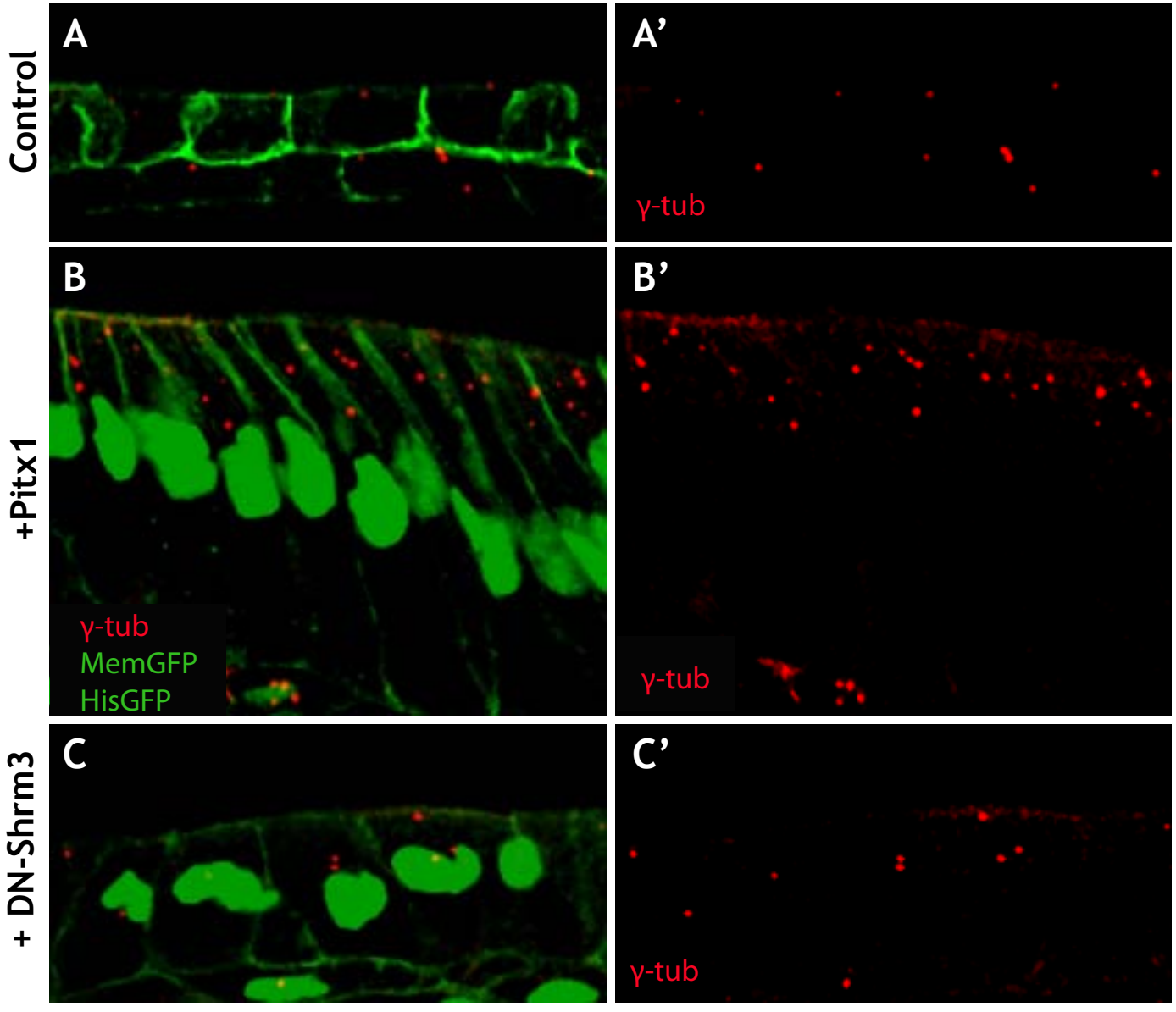
Control
+Pitx1
+Pitx1
+ DN-Shrm3
A
A'
γ-tub
B
B'
γ-tub
MemGFP
HisGFP
γ-tub
C
C'
γ-tub